Synthesis and Characterization of Thermally Stable Nanotubular TiO2 and Its Photocatalytic Activity

ARTICLE *in* THE JOURNAL OF PHYSICAL CHEMISTRY C · NOVEMBER 2008

Impact Factor: 4.77 · DOI: 10.1021/jp8031258

8 AUTHORS, INCLUDING:

Weiping Huang
Nankai University
122 PUBLICATIONS **2,866** CITATIONS

Synthesis and Characterization of Thermally Stable Nanotubular TiO_2 and Its Photocatalytic Activity

Huiqin An, Baolin Zhu, Junxia Li, Jian Zhou, Shurong Wang, Shoumin Zhang, Shihua Wu, and Weiping Huang*

Department of Chemistry, Nankai University, Tianjin 300071, China

Received: April 9, 2008; Revised Manuscript Received: September 28, 2008

Hydrogen titanate nanotubes obtained by hydrothermal synthesis are treated with sol containing titanium. The products are characterized with transmission electron microscopy, X-ray diffraction, thermal gravimetric analysis, and Raman spectroscopy. Their photocatalytic performance is evaluated by the photocatalytic degradation rates of methyl orange in aqueous solution under UV−vis light irradiation. The results reveal that the treated nanotubes are more thermally stable and exhibit better photocatalytic performance than primary nanotubes. The treated nanotubes can keep a tubular structure when calcined at 400 °C. However, their precursors collapse when they are calcined only at 300 °C. The more thermally stable new functional TiO_2 nanotubes can be prepared by using sol containing other elements instead of sol containing Ti in the future.

Introduction

Titanium dioxide has been extensively employed as a photocatalytic material for the purification and treatment of both contaminated air and water owing to its low cost, nontoxicity, and stability.[1−7] Particularly, TiO_2 nanotubes are expected to have some improved properties for photocatalytic applications.[8−12] The tubular structure, large surface-to-volume ratio, high sedimentation rate, and so on are the exceptional properties of TiO_2 nanotubes, which make TiO_2 nanotubes more suitable to be utilized as a catalyst or catalyst support for heterogeneous catalytic reactions.[9−12] These advantages drive people studying the synthesis and characterization of TiO_2 nanotubes intensively.[8−17] Lakshmi et al. synthesized TiO_2 nanotubes using porous alumina and polymeric filter membranes as the templates.[18] Peng et al. prepared TiO_2 nanotubes by using LAHC as the template in the LAHC/TBOT system.[19] Grimes and co-workers fabricated titanium oxide nanotubes by anodic oxidation of a pure titanium sheet in an aqueous solution containing 0.5−3.5 wt % hydrofluoric acid.[20] Bavykin et al. summarized the methods for preparation of TiO_2 nanotubes, compared possible crystal structures and mechanisms of formation of nanostructured TiO_2 and titanates, and reviewed their applications in catalysis, photocatalysis, electrocatalysis, lithium batteries, hydrogen storage, and solar-cell technologies.[21] One of the methods for preparing titanate nanotubes is simple hydrothermal treatment of TiO_2 powder in a 10 M NaOH aqueous solution and subsequent washing with HCl aqueous solution.[22] The synthesis process is a cheap one-step reaction, which requires neither expensive apparatus nor special chemicals. However, the obtained tubes have bad thermal stability and low photoefficiency in photocatalytic reaction,[23,24] which limits their practical applications. To overcome the obstacles mentioned above, many efforts have been made to modify TiO_2 nanotubes or explore new TiO_2 nanotubes-based systems from the point of practical use.[25,26] In this paper, we report synthesis of more thermal stable TiO_2 nanotubes by treating hydrogen titanate nanotubes with sol containing titanium.

* Corresponding author. E-mail: huangw@eyou.com. Telephone: +86-22-23502996.

Experimental Section

Materials. All the reagents are analytical grade and used without any further purification.

Characterization. The samples are characterized with transmission electron microscopy (TEM, Philips T20ST), X-ray diffraction (XRD, Rigaku D/Max-2500 X-ray diffractometer with Cu Kα radiation), thermal gravimetric analysis (TGA, ZPR-2P, 10 °C /min), and Raman spectroscopy (Nd:YAG laser ware).

Catalytic Activity Test. Photocatalytic activity experiments of the specimens used as photocatalysts for the degradation of methyl orange in water are performed in a UV-light reactor. Photocatalyst (0.05 g) is dispersed in 100 mL of methyl orange aqueous solution (17 mg/L) in each experiment. The reactor is illuminated with a 300 W high-pressure mercury lamp. At regular time intervals of illumination, a sample of mixture is collected and centrifuged, and the methyl orange concentration of clear solution is measured using a TU-1901 UV−vis spectrometer at 463.8 nm, which is the maximum absorption wavelength of methyl orange. The results are corrected for the decomposition of the dye in the absence of catalysts and for adsorption of dye on the catalyst.

Synthesis of Hydrogen Titanate Nanotubes. Hydrogen titanate nanotubes are synthesized with the method initially developed by Kasuga et al.[22] Pure anatase TiO_2 powder is dispersed in an aqueous solution of NaOH (10 M) and charged into a Teflon-lined autoclave. The autoclave is heated in an oil bath at 150 °C for 12 h. The prepared sample is washed with 0.1 M HNO_3 solution.

Treatment of Primary Nanotubes with Sol Containing Titanium. The solution of butyl titanate in absolute ethanol is prepared under vigorous stirring at the volume ratio of 1:15 (solution A). The solution of distilled water, absolute ethanol, and nitric acid (4 mol/L) is prepared at the volume ratio of 1:15:0.3 (solution B). Solution A is slowly dropped into solution B under continued stirring for 0.5 h (solution C). Then the hydrogen titanate nanotubes are dispersed in solution C under stirring for 12 h. After low-energy sonication for 3.5 h, the product is filtered, dried at 80 °C overnight, and then calcined at 200, 300, 400, and 500 °C, respectively, for 2 h.

10.1021/jp8031258 CCC: $40.75
Published on Web 11/06/2008

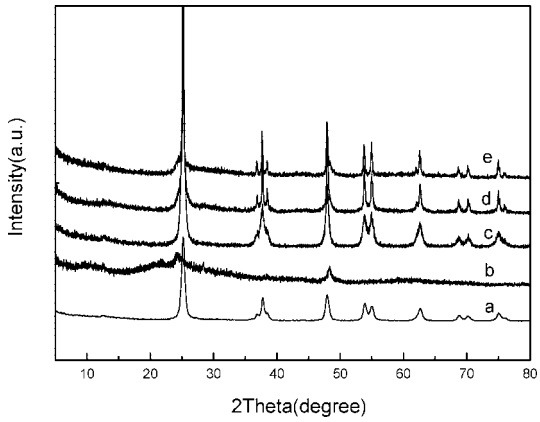

Figure 1. XRD patterns of calcined hydrogen titanate nanotubes at 400 °C (a) and sol-treated nanotubes calcined at 200 °C (b), 300 °C (c), 400 °C (d), and 500 °C (e).

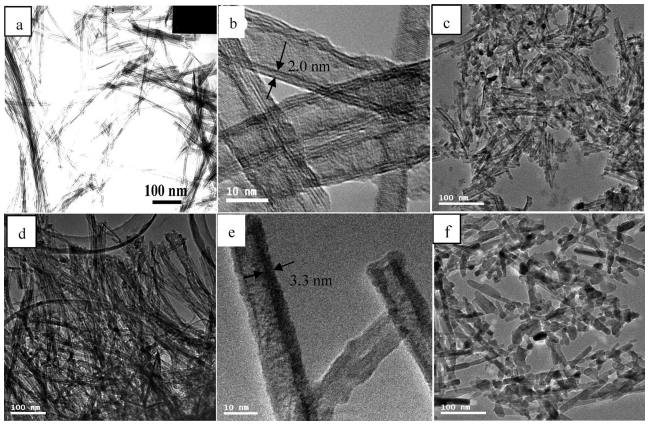

Figure 2. TEM images of as-prepared hydrogen titanate nanotubes (a, b), heated at 400 °C (c), and sol-treated nanotubes calcined at 400 °C (d, e) and 500 °C (f).

Results and Discussion

Characterization of Materials. Figure 1 depicts the XRD patterns of hydrogen titanate nanotubes and sol-treated nanotubes calcined at different temperatures. As shown in Figure 1a, the calcined nanotubes possess the anatase phase of TiO_2 (JCPDS 21-1272). Its specific peak is sharper and its half-width is narrower compared with those of sol-treated nanotubes (Figure 1b, c, and d). XRD patterns of sol-treated nanotubes (Figure 1b, c, d, and e) show the all main characteristic peaks of TiO_2. But there are some differences between them. For Figure 1b, peaks at 25.43° and 48.09° corresponding to the (101) and (200) crystal planes of anatase TiO_2 are not obvious and peak intensity is weak, and other peaks of anatase TiO_2 are absent, which means that amorphous titanate nanotubes do not turn into anatase phase completely. For Figure 1c, d, and e, all peaks corresponding to anatase phase are found and peak intensity increases with the increase of calcination temperature. That indicates that the anatase phase of TiO_2 forms and crystal phase becomes better with the increase of calcination temperature. From the half-width of the XRD peaks, we can judge that the average size of particles coating on sol-treated nanotubes becomes larger with the increase of calcination temperature.

Figure 2 shows the TEM images of hydrogen titanate nanotubes and sol-treated nanotubes calcined at different temperatures. Among them, the difference is obvious. As has been reported, hydrogen titanate nanotubes are open-ended, their diameters are nearly uniform, their length is more than hundreds of nanometers (Figure 2a), and their walls are multilayer with

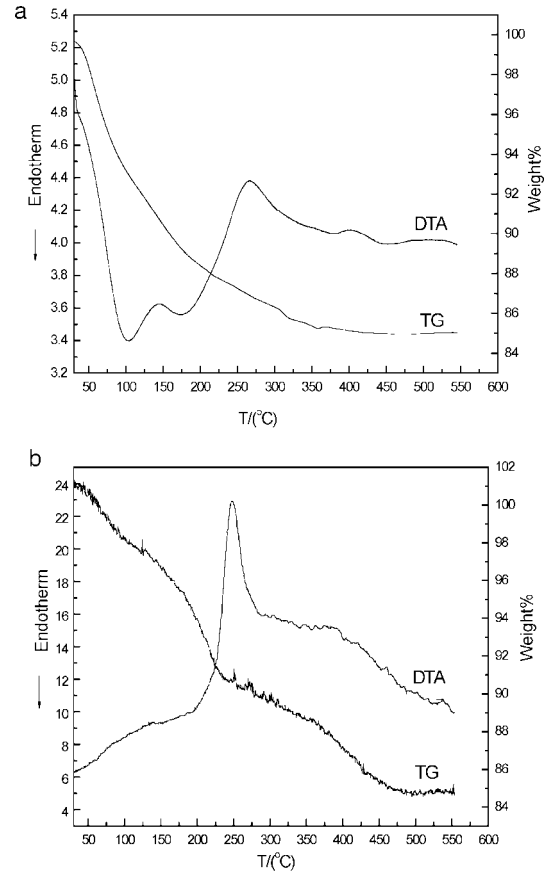

Figure 3. TG-DTA curves of hydrogen titanate nanotubes (a) and as-prepared sol-treated nanotubes (b).

an interlayer spacing of about 0.7 nm (Figure 2b).[27] The morphology of hydrogen titanate nanotubes calcined at 400 °C is displayed in Figure 2c. Compared with Figure 2a, it can be seen that the tubular structure of the sample has changed greatly, the length of the nanotubes is relatively short, and many lamellar particles support on linear bundles after the calcined process. On the other hand, the TEM images of sol-treated nanotubes (Figure 2d and e) show that the diameters of sol-treated nanotubes are in the range of 8−10 nm, and their lengths are up to several hundreds of nanometers. Many small particles are uniformly coated on the walls of tubes and inserted into the space of the interlayer. These particles are TiO_2 particles coming from the decomposition of sol. From Figure 2e, we can see that interlayer structure is not well-resolved and a solid wall forms. It is these particles that help support the nanotubular structure and make sol-treated nanotubes own higher thermal stability. Compared with hydrogen titanate nanotubes calcined under the same conditions (Figure 2c), the sol-treated nanotubes can withstand calcination at 400 °C (Figure 2d). However, the hydrogen titanate nanotubes collapse under the same conditions (Figure 2c). After calcination at 500 °C, some sol-treated nanotubes break (Figure 2f), and agglomeration occurs. It is in accordance with the decrease of the photocatalytic activity.

The TG-DTA curves of untreated and as-prepared sol-treated nanotubes are shown in Figure 3. It can be seen clearly that for untreated nanotubes there is a monotonic weight loss in the temperature range of room temperature to 350 °C (Figure 3a), which is in accordance with the literature.[23] The weight loss consists of two parts: one is physically adsorbed water and intralayered water, which corresponds to the endothermic peak on the DTA curve; the other is the dehydration of the interlayered OH group at about 300 °C, which corresponds to

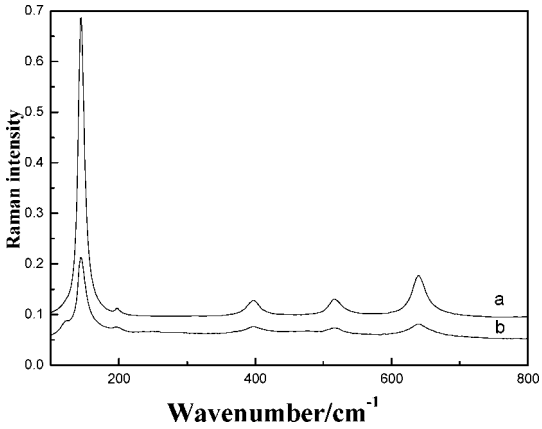

Figure 4. Raman spectra of hydrogen titanate nanotubes (a) and sol-treated nanotubes (b) calcined at 400 °C.

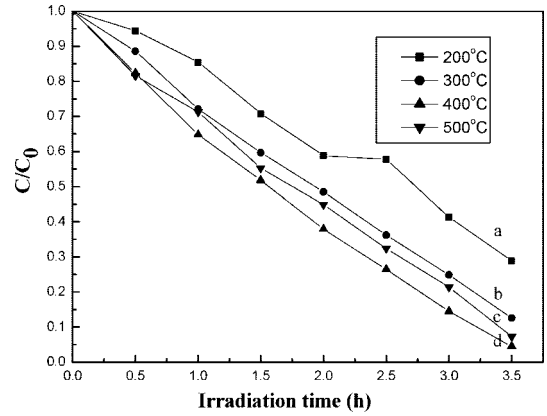

Figure 5. Photocatalytic activity of sol-treated nanotubes calcined at various temperatures.

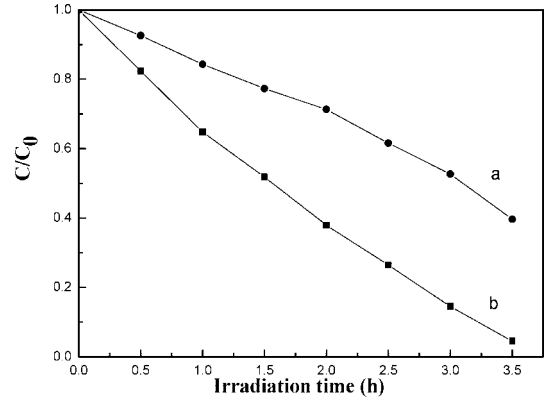

Figure 6. Photocatalytic activity of calcined hydrogen titanate nanotubes (a) and sol-treated nanotubes (b) at 400 °C.

the exothermic peak on the DTA curve. The results of TG-DTA and XRD reveal that the transition of the crystal phase from amorphous to anatase is exothermic and hydrogen titanate nanotubes are converted into TiO_2 nanoparticles completely after 350 °C, which is confirmed by the TEM image. Behind 350 °C the weight loss is not obvious. For the sol-treated TiO_2 nanotubes (Figure 3b), upon heating, the amorphous materials become crystalline and weight loss occurs. The TG curve could be divided into two main stages during the weight loss process. The first one takes place between 20 and 200 °C. In this process, all physically adsorbed material, e.g., water and ethanol, is removed. The second weight loss in the range of 200−450 °C can be attributed to loss of water and combustion of the remaining organic compounds, e.g., butanol and ethanol, accompanied with crystallization, which agrees with the exothermal peak of the DTA curve.[28] After 450 °C, the weight loss is not obvious.

Figure 4 presents Raman spectra of hydrogen titanate nanotubes and sol-treated nanotubes calcined at 400 °C. Both Raman peaks are similar. The Raman lines at 146, 394, 511, and 635 cm^{-1} can be assigned to the E_g, B_{1g}, A_{1g} or B_{2g}, and E_g modes of the anatase phase, respectively. The strongest E_g mode at 146 cm^{-1}, arising from the extension vibration of the anatase structure, is well-resolved, which indicates that the samples are anatase phase.[29,30] Upon examining the Raman spectra, we can see that there is no difference in the configuration between calcined hydrogen titanate nanotubes and sol-treated nanotubes.

Photocatalytic Activity of the Prepared Catalysts. The photocatalytic activities of the samples are evaluated by measuring the degradation of methyl orange in aqueous solution under UV light irradiation. Figure 5 shows the effects of calcination temperature on the photocatalytic degradation of methyl orange for sol-treated nanotubes. It is obvious that calcination temperature has a strong influence on the photoactivity of sol-treated nanotubes. From 200 to 400 °C (Figure 5a, b, and d), it can be observed that the photocatalytic activity increases with the increasing of calcination temperature and reaches a maximum value at 400 °C (Figure 5d). Compared with that of Figure 5d, the photocatalytic activity of sample calcined at 500 °C decreases (Figure 5c). In the photocatalytic reaction, anatase phase and surface area dominate the main effect.[31] From 200 to 400 °C, amorphous TiO_2 gradually turns into anatase TiO_2 and the surface area does not decrease obviously as the tubular structure exists, and the enhancement of crystallization of anatase raises the photocatalytic activity of sol-treated nanotubes. When the calcination temperature is 400 °C, there is the highest amount of anatase and still perfect nanotubular structure. So it has the highest photocatalytic activity. However, when the calcination temperature is 500 °C, a lot of nanotubes are broken. The length of the nanotubes becomes short, and the surface-to-volume ratio becomes small, which leads to the lower photocatalytic efficiency.

In comparison with hydrogen titanate nanotubes, Figure 6 shows the photocatalytic activity of hydrogen titanate nanotubes and sol-treated nanotubes calcined at 400 °C. After irradiation for 3.5 h, only 60% of the methyl orange is degraded in the presence of hydrogen titanate nanotubes, while in the presence of sol-treated nanotubes, 60% of the methyl orange is degraded after irradiation for only 2.0 h, and 100% is absolutely degraded after irradiation for 3.5 h. It can be seen that sol-treated nanotubes exhibit better photocatalytic performance than do hydrogen titanate nanotubes. Here the main limiting factor that controls the photocatalytic efficiency is the tubular structure and large surface-to-volume ratio. After calcination at 400 °C, the hydrogen titanate nanotubes have changed greatly. The tubular structure breaks and the length of the nanotubes is relatively short, which leads to its small surface-to-volume ratio and low photocatalytic efficiency.

Conclusions

(1) Sol-treated nanotubes are synthesized by treating hydrogen titanate nanotubes with sol containing titanium. Compared with the precursors, the obtained sol-treated nanotubes show a higher thermal stability.

(2) The photocatalytic activity of sol-treated nanotubes is examined by the photodegradation of aqueous methyl orange. The experiments demonstrate that photocatalytic performance of sol-treated nanotubes is best after calcination at 400 °C.

(3) As a thermal stable material, sol-treated nanotubes can completely replace hydrogen titanate nanotubes to be used as a catalyst or catalyst support in the future.

Acknowledgment. This work was supported by 973 Program (2005CB623607) and the National Natural Science Foundation of China (grant number: 20771061).

References and Notes

(1) Inoue, T.; Fujishima, A.; Konishi, S.; Honda, K. *Nature* **1979**, *277*, 637.
(2) Anpo, M.; Shima, T.; Kodama, S.; Kubokawa, Y. *J. Phys. Chem.* **1987**, *91*, 4305.
(3) Hoffmann, M. R.; Martin, S. T.; Choi, W.; Bahnemann, D. W. *Chem. Rev.* **1995**, *95*, 69.
(4) Zhang, F. L.; Zhao, J. C.; Shen, T.; Hidaka, H.; Pelizzetti, E.; Serpone, N. *Appl. Catal., B* **1998**, *15*, 147.
(5) Chu, S. Z.; Inoue, S.; Wada, K.; Li, D.; Haneda, H.; Awatsu, S. *J. Phys. Chem. B* **2003**, *107*, 6586.
(6) Raja, P.; Bandara, J.; Giordano, P.; Kiwi, J. *Ind. Eng. Chem. Res.* **2005**, *44*, 8959.
(7) Arabatzis, I. M.; Stergiopoulos, T.; Andreeva, D.; Kitova, S.; Neophytides, S. G.; Falaras, P. *J. Catal.* **2003**, *220*, 127.
(8) Xu, J. C.; Lu, M.; Guo, X. Y.; Li, H. L. *J. Mol. Catal. A* **2005**, *226*, 123.
(9) Idakiev, V.; Yuan, Z. Y.; Tabakova, T.; Su, B. L. *Appl. Catal., A* **2005**, *281*, 149.
(10) Zhu, B. L.; Guo, Q.; Huang, X. L.; Wang, S. R.; Zhang, S. M.; Wu, S. H.; Huang, W. P. *J. Mol. Catal. A* **2006**, *249*, 211.
(11) Mor, G. K.; Shankar, K.; Paulose, M.; Varghese, O. K.; Grimes, C. A. *Nano Lett.* **2006**, *6*, 215.
(12) Quan, X.; Yang, S. G.; Ruan, X. L.; Zhao, H. M. *Environ. Sci. Technol.* **2005**, *39*, 3770.
(13) Sander, M. S.; Cote, M. J.; Gu, W.; Kile, B. M.; Tripp, C. P. *Adv. Mater.* **2004**, *16*, 2052.
(14) Chen, Y. S.; Crittenden, J. C.; Hackney, S.; Sutter, L.; Hand, D. W. *Environ. Sci. Technol.* **2005**, *39*, 1201.
(15) Macak, J. M.; Zlamal, M.; Krysa, J.; Schmuki, P. *Small* **2007**, *3*, 300.
(16) Lai, Y. K.; Sun, L.; Chen, Y. C.; Zhuang, H. F.; Lin, C. J.; Chin, J. W. *J. Electrochem. Soc.* **2006**, *153*, D123.
(17) Chu, S. Z.; Wada, K.; Inoue, S.; Todoroki, S. *Chem. Mater.* **2002**, *14*, 266.
(18) Lakshmi, B. B.; Patrissi, C. J.; Martin, C. R. *Chem. Mater.* **1997**, *9*, 2544.
(19) Peng, T. Y.; Hasegawa, A.; Qiu, J. R.; Hirao, K. *Chem. Mater.* **2003**, *15*, 2011.
(20) Gong, D.; Grimes, C. A.; Varghese, O. K.; Hu, W. C.; Singh, R. S.; Chen, Z.; Dickey, E. C. *J. Mater. Res.* **2001**, *16*, 3331.
(21) Bavykin, D. V.; Friedrich, J. M.; Walsh, F. C. *Adv. Mater.* **2006**, *18*, 2807.
(22) Kasuga, T.; Hiramatsu, M.; Hoson, A.; Sekino, T.; Niihara, K. *Langmuir* **1998**, *14*, 3160.
(23) Zhang, M.; Jin, Z. S.; Zhang, J. W.; Guo, X. Y.; Yang, J. J.; Li, W.; Wang, X. D.; Zhang, Z. J. *J. Mol. Catal. A: Chem.* **2004**, *217*, 203.
(24) Wang, X. D.; Yang, J. J.; Jin, Z. S. *Photogr. Sci. Photochem.* **2002**, *20*, 424.
(25) Li, H.; Zhu, B. L.; Feng, Y. F.; Wang, S. R.; Zhang, S. M.; Huang, W. P. *J. Solid State Chem.* **2007**, *180*, 2136.
(26) Zhang, X.; Zhang, F.; Chan, K. Y. *Mater. Chem. Phys.* **2006**, *97*, 384.
(27) Zhu, B. L.; Li, K. R.; Feng, Y. F.; Zhang, S. M.; Wu, S. H.; Huang, W. P. *Catal. Lett.* **2007**, *118*, 55.
(28) Huang, W. P.; Tang, X. H.; Felner, I.; Koltypin, Y.; Gedanken, A. *Mater. Res. Bull.* **2002**, *37*, 1721.
(29) Xu, C. Y.; Zhang, P. X.; Yan, L. *J. Raman Spectrosc.* **2001**, *32*, 862.
(30) (a) Halamus, T.; Wojciechowski, P. *Polym. Adv. Technol.* **2007**, *18*, 411. (b) Halamus, T.; Wojciechowski, P.; Bobowska, I. *Polym. Adv. Technol.* **2008**, *19*, 807.
(31) Wang, J.; Li, R. H.; Zhang, Z. H.; Zhang, X. D.; Sun, W.; Wang, H.; Xu, R.; Xing, Z. Q. *J. Chem. Technol. Biotechnol.* **2007**, *82*, 588.

JP8031258